Chapter 10
A New Strategy for Testing Cosmology with Simulations

Madhura Killedar, Stefano Borgani, Dunja Fabjan, Klaus Dolag, Gian Luigi Granato, Susana Planelles, and Cinthia Ragone-Figueroa

Abstract Structural properties of clusters of galaxies have been routinely used to claim either tension or consistency with the fiducial cosmological hypothesis, known as ΛCDM. However, standard approaches are unable to quantify the preference for one hypothesis over another. We advocate using a 'weighted' variant of approximate Bayesian computation (ABC), whereby the parameters of the strong lensing-mass scaling relation, α and β, are treated as the summary statistics. We demonstrate then, for the first time, the procedure for estimating the likelihood for observing α and β under the ΛCDM framework. We employ computer simulations for producing mock samples, and account for variation between samples for modelling the likelihood function. We also consider the effects on the likelihood, and consequential ability to compare competing hypotheses, if only simplistic computer simulations are available.

Key words: Bayesian statistics, ABC, Simulations, Cosmology, Galaxy clusters

M. Killedar (✉)
Universitäts-Sternwarte München, Ludwig Maximilians University, München, Germany
e-mail: killedar@usm.lmu.de

S. Borgani
Dipartimento di Fisica, Università di Trieste, Trieste, Italy
e-mail: borgani@oats.inaf.it

D. Fabjan
SPACE-SI, Slovenian Centre of Excellence for Space Sciences and Technologies, Aškerčeva 12, 1000 Ljubljana, Slovenia

K. Dolag
Universitaets-Sternwarte Muenchen, Scheinerstrasse 1, D-81679, Muenchen, Germany

G.L. Granato • S. Planelles
Dipartimento di Fisica dell'Universita di Trieste, Sezione di Astronomia, Via Tiepolo 11, I-34131 Trieste, Italy

C. Ragone-Figueroa
Instituto de Astronomia Teorica y Experimental (IATE), Consejo Nacional de Investigaciones Científicas y Tecnicas de la Republica Argentina (CONICET), Observatorio Astronomico, Universidad Nacional de Cordoba, Laprida 854, X5000BGR Cordoba, Argentina

10.1 Introduction

Our standard model of cosmology, ΛCDM, is one in which our universe is made up primarily of dark energy, has a large amount of dark matter, and only a small fraction of ordinary matter; it is currently undergoing a period of expansion and an expansion that is accelerating. This model appears to describe the contents and evolution of the universe very well, and has been determined through the analysis of several astrophysical objects and phenomena. One additional dataset with the potential to provide complementary information is the mass-structure of clusters of galaxies [1, 2, 22, 24]. These objects contain hundreds to thousands of galaxies, as well as hot gas and dark matter, and they gravitationally lens and distort the images of more distant galaxies.

Strong lensing efficiencies, as characterised by the effective Einstein radii (denoted θ_E) scale well with the mass of clusters at large over-densities [14]. If any given set of galaxy clusters sample are, in fact, stronger lenses than predicted by the ΛCDM model, they will have larger θ_E for a given total mass at low over-densities (e.g., M_{500}). The earliest studies of similar galaxy-cluster properties revealed a significant difference between the observations and ΛCDM predictions [1, 15]. Thus began the hunt for solutions to the so-called tension with ΛCDM cosmology.

Previous works in the literature have claimed either 'tension' or 'consistency' with ΛCDM, or insufficient data [6, 11, 18, 21, 23, 27], but do not allow one to compare competing cosmological hypotheses. In the present work, we propose a Bayesian approach to the cosmological test using galaxy cluster strong lensing properties.

10.2 The Bayesian Framework

A Bayesian approach is advocated, in which one determines the relative preference of two hypothetical cosmological models, C_1 and C_2, in light of the data D, by calculating the Bayes factor B:

$$B = \frac{\mathscr{L}(D|C_1)}{\mathscr{L}(D|C_2)} \tag{10.1}$$

where $\mathscr{L}$ denotes the likelihood of the data assuming a cosmology.

The aim then is to calculate, under one chosen hypothesis: ΛCDM, the likelihood of observing the structural properties of a particular sample of galaxy clusters. This sample is detected using a well-defined selection criteria and all relevant properties have been measured [5, 7, 13, 16, 17, 26, 27].

10.2.1 Weighted ABC

Achieving the aforementioned goal is non-trivial, because a likelihood function related to the original observables (θ_E and M_{500}) is intractable. This is because: (a) computer simulations are deemed necessary for describing the irregular structure of galaxy clusters, which undergo non-linear structure formation; (b) there are a finite (and relatively small) number of clusters that can be simulated in a reasonable amount of time, and thus the full θ_E–M_{500} space cannot be sampled. Therefore, this problem is an ideal case for which one may apply a variant of approximate Bayesian computation (ABC) [4, 25]. What we propose is not a likelihood-free approach, however, and rather than rejecting mock samples that are dissimilar to the real data, they are down-weighted. Thus, we refer to the novel approach described below as Weighted ABC.

We assume a power-law relation between the strong lensing and mass proxies, and perform a fitting to the following function in logarithmic space[1]:

$$\log \left[\frac{M_{500}}{9 \times 10^{14} M_\odot} \right] = \alpha \log \left[\frac{\theta_E}{20"} \sqrt{\frac{D_d}{D_{ds}}} \right] + \beta \tag{10.2}$$

with parameters α and β, and aim to find the likelihood of observing *the scaling relationship*. α and β act as summary statistics for the dataset. However, rather than calculating precise values for α and β, one would determine a probability distribution that reflects the degree of belief in their respective values. The relevant fitting procedure is described in Sect. 10.2.2.

Next, we outline how to calculate the likelihood of observing α and β. In the following, ι represents background information such as knowledge of the cluster selection criteria, the method of characterising the Einstein radius, and the assumption that there exists a power-law relation between strong lensing and mass.

1. Computer simulations (see [3, 14, 19, 20]) are run within the framework of a chosen cosmological hypothesis, C. In our case, C represents the assumption that ΛCDM (or specific values for cosmological parameters) is the true description of cosmology.
2. Simulated galaxy clusters are selected according to specified criteria, ideally reflecting the criteria used to select the real clusters.
3. Different on-sky projections of these three-dimensional objects produce different apparent measurements of structural properties. Therefore, we construct a large

---

[1]The pivot mass $9 \times 10^{14} M_\odot$ is chosen to approximate the logarithmic average of the observed and simulated clusters. Similarly, the pivot Einstein radius is chosen to be 20 arcseconds. D_d represents the angular diameter distance from an observer on Earth to the galaxy cluster lens, while D_{ds} represents the angular diameter distance from the galaxy cluster lens to a more distant galaxy, in our case chosen to be fixed to a redshift of $z = 2$.

number of mock samples from these by randomly choosing an orientation-angle for each cluster. Equation (10.2) is fit to each mock sample (See Sect. 10.2.2), to determine a posterior over α and β: $P_i(\alpha, \beta | C, \iota)$ denotes the result for the ith of N mock samples. We combine these, to give the probability, $P(\alpha, \beta | C, \iota) \equiv \sum_{i=1}^{N} P_i(\alpha, \beta | C, \iota)$, that one would observe the scaling relation $\{\alpha, \beta\}$ under the hypothesis C. The result can be interpreted as a likelihood function *as a function of data*: α and β.

4. Fit Eq. (10.2) to the data to obtain the posterior probability distribution for α and β, $P(\alpha, \beta | \iota)$. The normalised posterior is then interpreted as a single 'data point': the distribution represents the uncertainty on the measurement of α and β.

5. Calculate the likelihood, $\mathscr{L}$, of observing the α–β fit as we did, by integrating over the product of the two aforementioned posteriors—now re-labelled 'data-point' and 'likelihood function'.

The result of integrating the product of $P(\alpha, \beta | C, \iota)$ and $P(\alpha, \beta | \iota)$ for the dataset is mathematically equivalent to integrating the product for each mock separately, then taking the average over all mock samples:

$$\int \left[\frac{1}{N} \sum_{i=1}^{N} P_i(\alpha, \beta | C, \iota) \right] P(\alpha, \beta | \iota) \, d\alpha \, d\beta = \frac{1}{N} \sum_{i=1}^{N} \int P_i(\alpha, \beta | C, \iota) P(\alpha, \beta | \iota) \, d\alpha \, d\beta \tag{10.3}$$

Thus, what we have described above is equivalent to the weighting of each mock sample according to its similarity to the real data, where the metric is the convolution of the two (mock and real) posterior probability distributions $P(\alpha, \beta | \iota)$.

10.2.2   Summary Statistic Fitting

The summary statistics α and β are parameters of the scaling relation between strong lensing efficiency and total cluster mass [Eq. (10.2)]. The procedure for calculating $\mathscr{L}$, as described in Sect. 10.2.1, requires one to fit real or mock data to determine the posterior distribution on α and β. We employ the Bayesian linear regression method outlined in [10]. Additionally, we acknowledge that intrinsic scatter is likely to be present, and thus introduce a nuisance parameter, V, which represents intrinsic Gaussian variance orthogonal to the line.

For this subsection, we change notation in order to reduce the subscripts: the mass of the i-th cluster lens as M_i, and the scaled Einstein radius as E_i. Each data-point is denoted by the vector $\mathbf{Z}_i = [\log M_i, \log E_i]$. Their respective uncertainties (*on the logarithms*) are denoted σ_M^2 and σ_E^2. Since we assume the uncertainties for Einstein radii and cluster mass are uncorrelated, the covariance matrix, $\mathbf{S}_i$, reduces to:

$$\mathbf{S}_i \equiv \begin{pmatrix} \sigma_M^2 & 0 \\ 0 & \sigma_E^2 \end{pmatrix} \tag{10.4}$$

In the case of a mock sample of simulated clusters, $\mathbf{S}_i = 0$.

Consider now the following quantities: $\varphi \equiv \arctan \alpha$, which denotes the angle between the line and the x-axis, and $b_\perp \equiv \beta \cos \varphi$ which is the orthogonal distance of the line to the origin. The orthogonal distance of each data-point to the line is:

$$\Delta_i = \hat{\mathbf{v}}^\top \mathbf{Z}_i - \beta \cos \varphi \tag{10.5}$$

where $\hat{\mathbf{v}} = [-\sin \varphi, \cos \varphi]$ is a vector orthogonal to the line.

Therefore, the orthogonal variance is

$$\Sigma_i^2 = \hat{\mathbf{v}}^\top \mathbf{S}_i \hat{\mathbf{v}}. \tag{10.6}$$

Following [10], we calculate the likelihood over the three-dimensional parameter space: $\Theta_1 \equiv \{\alpha, \beta, V\}$:

$$\ln \mathscr{L} = \mathrm{K} - \sum_{i=1}^{N} \frac{1}{2} \ln(\Sigma_i^2 + V) - \sum_{i=1}^{N} \frac{\Delta_i^2}{2\Sigma_i^2 + V} \tag{10.7}$$

where K is an arbitrary constant, and the summation is over all clusters in the considered sample.

While we ultimately (aim to) provide the parameter constraints on α and β, flat priors for these tend to unfairly favour large slopes. A more sensible choice is flat for the alternative parameters φ and $b_\perp$. We apply a modified Jeffreys prior on V:

$$\pi(V) \propto \frac{1}{V + V_t} \tag{10.8}$$

This is linearly uniform on V for small values and logarithmically uniform on V for larger values with a turnover, V_t, chosen to reflect the typical uncertainties.

Thus, for each Θ_1, we may define an alternative set of parameters $\Theta_2 \equiv \{\varphi, b_\perp, V\}$, for which the prior is given by:

$$\pi(\Theta_2) = \pi(\varphi, b_\perp)\pi(V)$$
$$\propto \pi(V) \tag{10.9}$$

where $\pi(V)$ is given by Eq. 10.8. The prior on Θ_1 is then dependent on the magnitude of the Jacobian of the mapping between the two sets of parameters:

$$\pi(\Theta_1) = \pi(\Theta_2)\det\frac{\partial \Theta_2}{\partial \Theta_1}$$
$$\equiv \pi(\Theta_2) \frac{1}{(1+\alpha^2)^{3/2}} \tag{10.10}$$

Boundaries on the priors are sufficiently large[2]: $-8 \leq \beta \leq 8$; $-40 \leq \alpha \leq 40$; $0 \leq V \leq V_{\text{max}}$. V_{max} is chosen to reflect the overall scatter in the data. The posterior is calculated following Bayes' theorem:

$$P(\Theta_1|D) \propto \mathscr{L}(D|\Theta_1)\,\pi(\Theta_1) \tag{10.11}$$

and is normalised. In practice, the posterior distribution was sampled by employing `emcee` [8], the python implementation of the affine-invariant ensemble sampler for Markov chain Monte Carlo (MCMC) proposed by [9].

As we are interested in the constraints on α and β, we then marginalise over the nuisance parameter, V.

10.3 Results

In Fig. 10.1, we show the relation between the Einstein radii and the cluster mass M_{500}. The real cluster sample is represented by red circles. For simulated clusters, the situation is more complicated. Since different lines of sight provide a large variation in projected mass distribution, each cluster cannot be associated with an individual Einstein radius, nor a simple Gaussian or log-normal distribution [14]. We therefore measure the Einstein radius for 80 different lines of sight and, for ease of visualisation, describe the distribution of Einstein radii for each simulated cluster by a box-plot.

Fig. 10.1 Strong lensing efficiency, characterised by scaled Einstein radii, $\theta_{\text{E,eff}}$, plotted as a function of mass. The range of Einstein radii for simulated clusters are shown by the *blue box-plots*. The *red circles* represent the real clusters. The *red line* marks the maximum a-posteriori fit to observational data, while the *thin blue lines* mark the fit to 20 randomly chosen mock samples from simulations

---
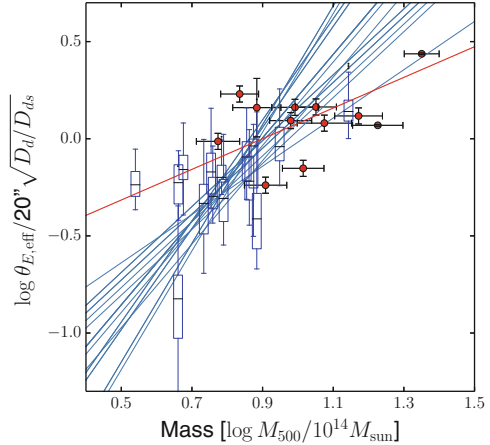
[2]The physically motivated choice of restricting $\alpha \geq 0$ is also explored; however, this has very minor effects on the final results despite removing the (small) secondary peak in the marginal posterior on α and β.
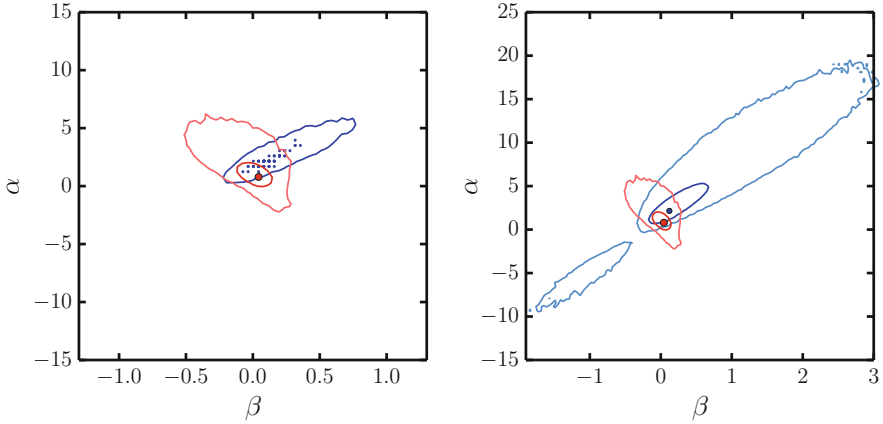
Fig. 10.2 *Left*: 1-σ and 2-σ constraints on parameters of the strong lensing—mass relation given the real cluster data (*red contours*), with a maximum a posteriori fit marked by a *red circle*. Overplotted in *blue dots* are the best fits to 80 mock observations of simulated galaxy clusters. A typical 1-σ error is shown as a *blue ellipse*. *Right*: Same as the middle panel, but the *blue circle* and *curves* mark, respectively, the maximum and the 1-σ and 2-σ contours of the likelihood function found by combining all 80 mocks. Ultimately, the likelihood, $\mathcal{L} \approx 0.3$, is found by convolving the functions marked by the *red* and *blue contours*

We fit the observational data to the lensing-mass relation and after marginalising out the nuisance parameter, V, present the posterior distribution for α and β, denoted by red contours in the left-hand panel of Fig. 10.2. This fit is reinterpreted as a single 'data-point'. To estimate the likelihood, *as a function of possible data*, we employ simulations. Many mock samples are individually fit to the lensing-mass relations; the maximum of the posterior is shown as a blue point and a typical 1-σ error shown as a blue ellipse. By adding the posteriors for each mock sample and renormalising, we estimate the required likelihood function, shown by the blue contours in the right-hand panel of Fig. 10.2. By multiplying by the 'data-point' distribution and integrating over the parameter space, we find $\mathcal{L} \approx 0.3$.

Note that one cannot comment on whether the likelihood is *large* or *small*. Currently, such simulations are only available for the fiducial ΛCDM cosmological model. However, if the same process is repeated for simulations under a different model, then the Bayes factor can be calculated [see Eq. (10.1)] and, after accounting for priors, may (or may not) reveal a preference for one of the cosmologies, in light of this data. Alternative cosmological models may include, for example, those with a different relative dark matter to dark energy ratio, interactions between the two dark components, or a different normalisation for the structure power spectrum.

10.4 Computational Challenge

The approach described above is an exciting new strategy for calculating the likelihood for observing strong lensing galaxy clusters for a chosen cosmological hypothesis. *However*, we recognise that the calculation involves running computer simulations that can take months. Computationally 'cheaper' simulations ignore several astrophysical processes in the formation of galaxy clusters and it is debatable whether these would be sufficient.

In order to determine the severity of this problem, we repeat the aforementioned procedure using galaxy cluster counterparts from such simulations, at varying levels of complexity and realism, and find that the likelihood, $\mathscr{L}$, can then vary by a factor of three or four. If the cheaper simulations are employed, then the selection criteria must also be replaced with an alternative compromise. We test this alternative and find that $\mathscr{L}$ changes by a factor of two.

Our findings suggest that if a model-comparison study was carried out using a simulation based on an alternative cosmological hypothesis and resulting in a Bayes factor of 20 or more [see Eq. (10.1)], then the cheaper simulations (or toy models based on these) would be sufficient. However, in the event that the Bayes factor B is found to be smaller, then the computationally expensive but realistic simulations would be necessary.

---

[3] http://www.python.org.

[4] http://www.numpy.org.

[5] http://www.scipy.org.

[6] http://roban.github.com/CosmoloPy/.

References

[1] Bartelmann, M., Huss, A., Colberg, J.M., Jenkins, A., Pearce, F.R.: Arc statistics with realistic cluster potentials. IV. Clusters in different cosmologies. A&A **330**, 1–9 (1998)

[2] Bartelmann, M., Meneghetti, M., Perrotta, F., Baccigalupi, C., Moscardini, L.: Arc statistics in cosmological models with dark energy. A&A **409**, 449–457 (2003). Doi:10.1051/0004-6361:20031158

[3] Bonafede, A., Dolag, K., Stasyszyn, F., Murante, G., Borgani, S.: A non-ideal MHD gadget: simulating massive galaxy clusters. ArXiv e-prints (2011)

[4] Cameron, E., Pettitt, A.N.: Approximate Bayesian computation for astronomical model analysis: a case study in galaxy demographics and morphological transformation at high redshift. MNRAS **425**, 44–65 (2012). Doi:10.1111/j.1365-2966.2012.21371.x

[5] Coe, D., Zitrin, A., Carrasco, M., Shu, X., Zheng, W., Postman, M., Bradley, L., Koekemoer, A., Bouwens, R., Broadhurst, T., Monna, A., Host, O., Moustakas, L.A., Ford, H., Moustakas, J., van der Wel, A., Donahue, M., Rodney, S.A., Benítez, N., Jouvel, S., Seitz, S., Kelson, D.D., Rosati, P.: CLASH: three strongly lensed images of a candidate z ≈ 11 galaxy. ApJ **762**, 32 (2013). Doi:10.1088/0004-637X/762/1/32

[6] Dalal, N., Holder, G., Hennawi, J.F.: Statistics of giant arcs in galaxy clusters. ApJ **609**, 50–60 (2004). Doi:10.1086/420960

[7] Ebeling, H., Barrett, E., Donovan, D., Ma, C.J., Edge, A.C., van Speybroeck, L.: A complete sample of 12 very X-ray luminous galaxy clusters at $z > 0.5$. ApJ Lett. **661**, L33–L36 (2007). Doi:10.1086/518603

[8] Foreman-Mackey, D., Hogg, D.W., Lang, D., Goodman, J.: emcee: the MCMC hammer. PASP **125**, 306–312 (2013). Doi:10.1086/670067

[9] Goodman, J., Weare, J.: Ensemble samplers with affine invariance. App. Math. Comput. Sci. **5**(1), 65–80 (2010)

[10] Hogg, D.W., Bovy, J., Lang, D.: Data analysis recipes: fitting a model to data. ArXiv e-prints (2010)

[11] Horesh, A., Maoz, D., Hilbert, S., Bartelmann, M.: Lensed arc statistics: comparison of millennium simulation galaxy clusters to hubble space telescope observations of an X-ray selected sample. MNRAS **418**, 54–63 (2011). Doi:10.1111/j.1365-2966.2011.19293.x

[12] Hunter, J.D.: Matplotlib: a 2d graphics environment. Comput. Sci. Eng. **9**(3), 90–95 (2007)

[13] Johnson, T.L., Sharon, K., Bayliss, M.B., Gladders, M.D., Coe, D., Ebeling, H.: Lens models and magnification maps of the six hubble Frontier fields clusters. ArXiv e-prints (2014)

[14] Killedar, M., Borgani, S., Meneghetti, M., Dolag, K., Fabjan, D., Tornatore, L.: How baryonic processes affect strong lensing properties of simulated galaxy clusters. MNRAS **427**, 533–549 (2012). Doi:10.1111/j.1365-2966.2012.21983.x

[15] Li, G.L., Mao, S., Jing, Y.P., Bartelmann, M., Kang, X., Meneghetti, M.: Is the number of giant arcs in ΛCDM consistent with observations? ApJ **635**, 795–805 (2005). Doi:10.1086/497583

[16] Mantz, A., Allen, S.W., Ebeling, H., Rapetti, D., Drlica-Wagner, A.: The observed growth of massive galaxy clusters - II. X-ray scaling relations. MNRAS **406**, 1773–1795 (2010). Doi:10.1111/j.1365-2966.2010.16993.x

[17] Medezinski, E., Umetsu, K., Nonino, M., Merten, J., Zitrin, A., Broadhurst, T., Donahue, M., Sayers, J., Waizmann, J.C., Koekemoer, A., Coe, D., Molino, A., Melchior, P., Mroczkowski, T., Czakon, N., Postman, M., Meneghetti, M., Lemze, D., Ford, H., Grillo, C., Kelson, D., Bradley, L., Moustakas, J., Bartelmann, M., Benítez, N., Biviano, A., Bouwens, R., Golwala, S., Graves, G., Infante, L., Jiménez-Teja, Y., Jouvel, S., Lahav, O., Moustakas, L., Ogaz, S., Rosati, P., Seitz, S., Zheng, W.: CLASH: complete lensing analysis of the largest cosmic lens MACS J0717.5+3745 and surrounding structures. ApJ **777**, 43 (2013). Doi:10.1088/0004-637X/777/1/43

[18] Meneghetti, M., Fedeli, C., Zitrin, A., Bartelmann, M., Broadhurst, T., Gottlöber, S., Moscardini, L., Yepes, G.: Comparison of an X-ray-selected sample of massive lensing clusters with the MareNostrum Universe ΛCDM simulation.   A&A **530**, A17+ (2011). Doi:10.1051/0004-6361/201016040

[19] Planelles, S., Borgani, S., Fabjan, D., Killedar, M., Murante, G., Granato, G.L., Ragone-Figueroa, C., Dolag, K.: On the role of AGN feedback on the thermal and chemo-dynamical properties of the hot intracluster medium.   MNRAS **438**, 195–216 (2014). Doi:10.1093/mnras/stt2141

[20] Ragone-Figueroa, C., Granato, G.L., Murante, G., Borgani, S., Cui, W.: Brightest cluster galaxies in cosmological simulations: achievements and limitations of active galactic nuclei feedback models. MNRAS **436**, 1750–1764 (2013). Doi:10.1093/mnras/stt1693

[21] Sereno, M., Giocoli, C., Ettori, S., Moscardini, L.: The mass-concentration relation in lensing clusters: the role of statistical biases and selection effects. ArXiv e-prints (2014)

[22] Takahashi, R., Chiba, T.: Gravitational lens statistics and the density profile of Dark Halos. ApJ **563**, 489–496 (2001). Doi:10.1086/323961

[23] Waizmann, J.C., Redlich, M., Meneghetti, M., Bartelmann, M.: The strongest gravitational lenses: III. The order statistics of the largest Einstein radii. ArXiv e-prints (2014)

[24] Wambsganss, J., Bode, P., Ostriker, J.P.: Giant arc statistics in concord with a concordance lambda cold dark matter universe. ApJ Lett. **606**, L93–L96 (2004). Doi:10.1086/421459

[25] Weyant, A., Schafer, C., Wood-Vasey, W.M.: Likelihood-free cosmological inference with type ia supernovae: approximate bayesian computation for a complete treatment of uncertainty. ApJ **764**, 116 (2013). Doi:10.1088/0004-637X/764/2/116

[26] Zheng, W., Postman, M., Zitrin, A., Moustakas, J., Shu, X., Jouvel, S., Høst, O., Molino, A., Bradley, L., Coe, D., Moustakas, L.A., Carrasco, M., Ford, H., Benítez, N., Lauer, T.R., Seitz, S., Bouwens, R., Koekemoer, A., Medezinski, E., Bartelmann, M., Broadhurst, T., Donahue, M., Grillo, C., Infante, L., Jha, S.W., Kelson, D.D., Lahav, O., Lemze, D., Melchior, P., Meneghetti, M., Merten, J., Nonino, M., Ogaz, S., Rosati, P., Umetsu, K., van der Wel, A.: A magnified young galaxy from about 500 million years after the Big Bang. Nature **489**, 406–408 (2012). Doi:10.1038/nature11446

[27] Zitrin, A., Broadhurst, T., Barkana, R., Rephaeli, Y., Benítez, N.: Strong-lensing analysis of a complete sample of 12 MACS clusters at $z > 0.5$: mass models and Einstein radii. MNRAS **410**, 1939–1956 (2011). Doi:10.1111/j.1365-2966.2010.17574.x